Trajectory Tracking for a Magnetically Levitated Shaft with Three-Phase AMBs in Y-Connection

St. Eckhardt and J. Rudolph
Technische Universität Dresden
Institut für Regelungs- und Steuerungstheorie
01062 Dresden, Germany
{*stephan.eckhardt, joachim.rudolph*}@*tu-dresden.de*

***Abstract*— High precision tool path tracking with magnetically supported spindles is considered. If radial bearings with three phases in Y-connection are used standard commercial power electronics can be employed. However, only two independent currents are available then. It is shown how this problem can be overcome. Experimental results show that the tracking precision obtained with Y-connected coils is similar to the one obtained with three independent coils.**

I. Introduction

Use of active magnetic bearings to support the rotor in machine tool spindles allows one to produce non-circular holes. To this end the (single) cutting edge of the tool must follow a non-circular path, which is synchronous with the rotation and, moreover, may vary along the hole. As a result, a high precision trajectory tracking problem must be solved.

The background for this problem is an industrial demand for spindles which can follow synchronous paths with off-center positions of the order of 50 micro-meters. The precision required is very demanding, as path tracking errors must not exceed 1 micro-meter on circular paths and 3 micro-meters on non-circular ones. Typical rotational velocities are up to 10000 rpm. We have solved this problem in co-operation with Axomat GmbH during the last years (see [1], [3]).

In order to be able to compete with other types of spindles it is interesting to reduce the costs. It is, therefore, desired to use commercial power amplifiers (e.g. DC-voltage link inverters). This requires to account for the current constraints resulting from the Y-connection. From a control point of view, such a connection leads to the availability of only two rather than three independent control inputs per radial bearing. This aspect lies in the focus of the present contribution where we show how a controller can be designed which uses the (only) two independent currents available with the Y-connected coils.

II. Description of the Laboratory Device

A typical configuration used in our laboratory equipment is the following (see Fig. 1). The shaft (about 0.6 m long, 10 kg) is supported by two three-phase electromagnetic radial bearings (as sketched in Fig. 2) and a classical electromagnetic axial bearing which acts on a disc. The drive is an induction motor.

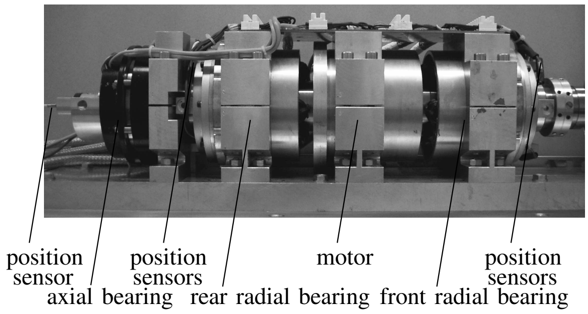

Fig. 1. Photograph of a laboratory spindle.

Position and orientation of the rotor are measured using two pairs of eddy current sensors in two planes perpendicular to the axis of symmetry and one such sensor along this axis. The angular position about the longitudinal axis is measured with a contactless incremental sensor. Using this information the tool trajectory is synchronized with the rotation. In our laboratory spindle the power amplifiers used are switched transistor bridges the duty ratios of which may serve as eight independent controls (3 per radial bearing, 2 on the axial one). This amplifier set-up allows us to compare such a three control configuration with the Y-connection on the same electronic hardware, as it is the aim of the present paper. Of course, if we are not interested in comparison we use alternative inverters. The computer hardware on the test-bench is a dSpace 1103.

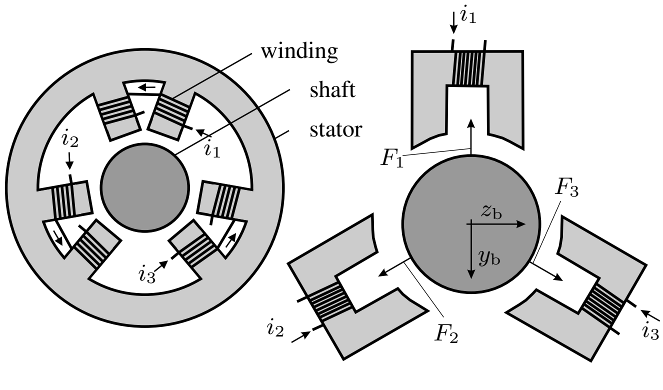

Fig. 2. Sketch of the three-phase radial bearing and simplified horseshoe type decoupled model.

III. Modeling

For the sake of completeness we sketch the main parts of the model. However, there is no need to account for the axial direction and the rotation about the spindle axis, these motions are decoupled. The position controller used for tool-path tracking is based on the following (reduced) rigid body model of the "mechanical part":

$$\begin{pmatrix} \ddot{Y} \\ \ddot{Z} \\ \ddot{\psi} \\ \ddot{\theta} \end{pmatrix} = M \begin{pmatrix} F_{y,+} \\ F_{z,+} \\ F_{y,-} \\ F_{z,-} \end{pmatrix} + \begin{pmatrix} g_y \\ g_z \\ 0 \\ 0 \end{pmatrix}$$

with the constant parameter matrix

$$M = \begin{pmatrix} \frac{1}{m} & 0 & \frac{1}{m} & 0 \\ 0 & \frac{1}{m} & 0 & \frac{1}{m} \\ 0 & \frac{-l_{\mathrm{b},+}}{J_2} & 0 & \frac{l_{\mathrm{b},-}}{J_2} \\ \frac{l_{\mathrm{b},+}}{J_2} & 0 & \frac{-l_{\mathrm{b},-}}{J_2} & 0 \end{pmatrix}$$

The forces involved in these equations are modeled by the standard static relation between bearing currents and air gap lengths ($j \in \{+,\ -\}, k \in \{1,\ 2,\ 3\}$ in this section):

$$F_{k,j} = \lambda_{k,j} \frac{i_{k,j}^2}{l_{j,k}^2} \tag{1}$$

with

$$l_{j,k} = s_j - \begin{pmatrix} \cos\alpha_{k,j} \\ \sin\alpha_{k,j} \end{pmatrix}^T \begin{pmatrix} Y_{\mathrm{b},j} \\ Z_{\mathrm{b},j} \end{pmatrix}$$

Here $Y_{\mathrm{b},j}, Z_{\mathrm{b},j}$ are the rotor axis positions in the bearing planes, s_j the nominal air gap lengths, and $\lambda_{k,j}$ are constant parameters depending on the bearing geometry and materials.

Each coil current generates a magnetic force, and the superposition of these three magnetic forces results in the bearing force vector

$$\begin{pmatrix} F_{y,j} \\ F_{z,j} \end{pmatrix} = \begin{pmatrix} \cos\alpha_{1,j} & \cos\alpha_{2,j} & \cos\alpha_{3,j} \\ \sin\alpha_{1,j} & \sin\alpha_{2,j} & \sin\alpha_{3,j} \end{pmatrix} \begin{pmatrix} F_{1,j} \\ F_{2,j} \\ F_{3,j} \end{pmatrix}$$

In case of Y-connected coils, the additional constraint

$$i_{1,j} + i_{2,j} + i_{3,j} = 0 \tag{2}$$

must be considered (in each bearing).

IV. Controller Design

The control is realized as a cascade, with a current controller in the inner and a position controller in the outer loop. The design of the position controller follows the flatness based control paradigm. Several types of solutions of this type have been proposed in the literature [2], [3]. The method relies on two facts that are characteristic for the class of so-called differentially flat nonlinear systems. Firstly, system trajectories can be parameterized by a finite set of independent trajectories of a so-called flat output. Secondly, the dynamics of the tracking errors of these flat output trajectories, i.e., their deviation from the desired trajectories, can be freely assigned. A typical approach uses linear time invariant error dynamics resulting in exponential convergence. Unlike the two references cited, at the last ISMB [1] we have proposed an alternative that uses a flat output consisting of the positions of the shaft in two planes perpendicular to the spindle symmetry axis. These planes can be freely chosen (typically the plane of the motion of the cutting edge and a plane somewhere at the other end of the rotor).

The flatness-based tracking controller has been discussed in detail in [1]–[3], and we do not repeat this here. Depending on the path tracking errors and their derivatives it calculates the forces required in the radial (and axial) bearings. This part of the computations does not depend on the type of bearings used. Based on these force requirements corresponding currents must be calculated. With the decoupled bearings considered here this can be done independently for each bearing. This will be detailed in the sequel. As similar relations must be considered (independently) in both bearings, there is no need to distinguish between the two bearings. Therfore, in order to simplify notation, we drop the index j used above. Moreover, again for the sake of simplicity, we consider a symmetrical design with

$$\alpha_1 = 0, \quad \alpha_2 = \frac{2\pi}{3}, \quad \alpha_3 = \frac{4\pi}{3}$$

A. Unconnected Coils: Three Controls

We consider the output of the position tracking controller to be the two Cartesian components of the resultant force in each bearing F_y, F_z. (Again, in order to keep notation simple we do not introduce indeces to distinguish the desired forces from those actually delivered.)

The decision about which forces to produce is taken depending on the signs of the forces required. However, as the two lower coils on the right of Fig. 2 produce a force in y-direction also the relevant force is

$$\hat{F}_y = F_y + \frac{|F_z|}{\sqrt{3}}$$

Based upon these considerations and the geometry of the bearing one gets the required forces from

$$\bar{F}_1 = \begin{cases} \hat{F}_y & \text{if } \hat{F}_y > 0 \\ 0 & \text{if } \hat{F}_y \le 0 \end{cases}$$

$$\bar{F}_2 = \begin{cases} \frac{2F_z}{\sqrt{3}} & \text{if } \hat{F}_y > 0,\ F_z > 0 \\ 0 & \text{if } \hat{F}_y > 0,\ F_z \le 0 \\ F_y + \sqrt{3}F_z & \text{if } \hat{F}_y \le 0,\ F_z > 0 \\ \hat{F}_y & \text{if } \hat{F}_y \le 0,\ F_z \le 0 \end{cases}$$

$$\bar{F}_3 = \begin{cases} 0 & \text{if } \hat{F}_y > 0,\ F_z > 0 \\ -\frac{2F_z}{\sqrt{3}} & \text{if } \hat{F}_y > 0,\ F_z \le 0 \\ \hat{F}_y & \text{if } \hat{F}_y \le 0,\ F_z > 0 \\ F_y - \sqrt{3}F_z & \text{if } \hat{F}_y \le 0,\ F_z \le 0 \end{cases}$$

Note that in any case at least one of the three forces $\bar{F}_1, \bar{F}_2, \bar{F}_3$ is zero. These forces are determined up to an additive force $F_0 \geq 0$ only. The resultant force is the same for any triple (F_1, F_2, F_3) satisfying

$$F_1 = \bar{F}_1 + F_0, \quad F_2 = \bar{F}_2 + F_0, \quad F_3 = \bar{F}_3 + F_0 \quad (3)$$

Finally, the three independent currents required to produce the forces F_1, F_2, F_3, and with these (F_y, F_z), can be calculated using the position dependent current-force relations (1), where we use $\lambda_k = \lambda, k = 1, 2, 3$ for simplicity:

$$i_k = \pm l_k \sqrt{F_k/\lambda}, \quad k = 1, 2, 3 \quad (4)$$

These currents are adjusted by an (inner-loop) current controller not further considered here.

B. Connected Coils: Two Controls

The resultant force (vector in the bearing plane) is generated from a triple of positive bearing forces determined up to the bias force $F_0 \geq 0$. The possibility to choose this free parameter is exploited in the control design. An appropriate choice of this parameter allows us to meet the algebraic constraint (2) due to the Y-connection of the coils: the sum of the three phase currents is zero.

Substituting (4) and (3) in (2) we get three possible configurations:

$$l_1 \sqrt{\bar{F}_1 + F_0} - l_2 \sqrt{\bar{F}_2 + F_0} + l_3 \sqrt{\bar{F}_3 + F_0} = 0 \quad (5a)$$
$$l_1 \sqrt{\bar{F}_1 + F_0} + l_2 \sqrt{\bar{F}_2 + F_0} - l_3 \sqrt{\bar{F}_3 + F_0} = 0 \quad (5b)$$
$$l_1 \sqrt{\bar{F}_1 + F_0} - l_2 \sqrt{\bar{F}_2 + F_0} - l_3 \sqrt{\bar{F}_3 + F_0} = 0 \quad (5c)$$

As observed in Section IV-A, we may distinguish three cases each identified by one of the forces $\bar{F}_k, k = 1, 2, 3$ being zero. It is, therefore, sufficient to discuss one of these cases, the other ones being treated similarly. We choose the case $\bar{F}_1 = 0$ for our discussion.

Using $\bar{F}_1 = 0$ in (5) and taking squares twice (on any of the three equations) yields a quadratic in F_0:

$$aF_0^2 + bF_0 + c = 0$$

In case $a = \left(l_1^2 + l_2^2 - l_3^2\right)^2 - 4l_1^2 l_2^2 \neq 0$ we get the roots

$$F_{0,1/2} = -\frac{p}{2} \pm \sqrt{\frac{p^2}{4} - q} \quad (6)$$

with

$$p = \frac{2\left(\left(l_2^2 - l_1^2 - l_3^2\right) l_2^2 \bar{F}_2 - \left(l_1^2 + l_2^2 - l_3^2\right) l_3^2 \bar{F}_3\right)}{\left(l_1^2 + l_2^2 - l_3^2\right)^2 - 4l_1^2 l_2^2}$$
$$q = \frac{\left(l_2^2 \bar{F}_2 - l_3^2 \bar{F}_3\right)^2}{\left(l_1^2 + l_2^2 - l_3^2\right)^2 - 4l_1^2 l_2^2}$$

In case $a = \left(l_1^2 + l_2^2 - l_3^2\right)^2 - 4l_1^2 l_2^2 = 0$ we get

$$F_0 = \frac{-\left(l_2^2 \bar{F}_2 - l_3^2 \bar{F}_3\right)^2}{2\left(\left(l_2^2 - l_1^2 - l_3^2\right) l_2^2 \bar{F}_2 - \left(l_1^2 + l_2^2 - l_3^2\right) l_3^2 \bar{F}_3\right)}$$

(Existence of solutions is discussed in the next subsection.)

Once $F_0 \geq 0$ has been determined the control currents can be calculated as above: substitute F_0 in (3) in order to get the forces $F_k, k = 1, 2, 3$ and compute three currents with (4). Though the signs of the currents do not influence the forces, in order to meet the Y-connection constraint (2), the sign is important. According to their absolute values, introduce new subscripts for the currents i_1, i_2, i_3 such that

$$|i_{\min}| \leq |i_{\text{med}}| \leq |i_{\max}|$$

Then the signs of the currents are chosen such that

$$i_{\min} = -\text{sign}\left(i_{\max}\right) |i_{\min}|$$
$$i_{\text{med}} = -\text{sign}\left(i_{\max}\right) |i_{\text{med}}|$$

C. Domain of Operation with Connected Coils

Above we have not discussed the existence of solutions of the problem, i.e., existence of the forces. Indeed this slightly restricts the domain of operation of the device. It can be discussed by considering the discriminant $\frac{p^2}{4} - q \geq 0$ which leads to:

$$\bar{F}_3^{\,2} l_3^2 + \bar{F}_2 \bar{F}_3 \left(-l_3^2 + l_1^2 - l_2^2\right) + \bar{F}_2^{\,2} l_2^2 \geq 0$$

Division by $\bar{F}_3^{\,2}$ yields a condition on $\bar{F}_2/\bar{F}_3$:

$$l_3^2 + \frac{\bar{F}_2}{\bar{F}_3}\left(-l_3^2 + l_1^2 - l_2^2\right) + \left(\frac{\bar{F}_2}{\bar{F}_3}\right)^2 l_2^2 \geq 0$$

There must not be any real roots. With

$$\frac{\left(-l_3^2 + l_1^2 - l_2^2\right)^2}{4l_2^4} - \frac{l_3^2}{l_2^2} < 0$$

this leads to

$$\left(l_1^2 - (l_2 + l_3)^2\right)\left(l_1^2 - (l_2 - l_3)^2\right) < 0$$

and

$$|l_2 + l_3| \geq l_1 \geq |l_2 - l_3|$$

Now the relation between the air gaps and the Cartesian coordinates

$$l_1 = l_0 + Y$$
$$l_2 = l_0 - \frac{1}{2}Y + \frac{\sqrt{3}}{2}Z$$
$$l_3 = l_0 - \frac{1}{2}Y - \frac{\sqrt{3}}{2}Z$$

and

$$|2l_0 - Y| \geq l_0 + Y \geq |\sqrt{3}Z|$$

allow us to recognize a triangular domain of operation determined by the conditions

$$\sqrt{3}Z - Y \leq l_0$$
$$-\sqrt{3}Z - Y \leq l_0$$
$$2Y \leq l_0$$

This result is illustrated by Fig. 3. Finally, it can also be shown that inside this domain of operation one of the solutions of (6) is non-negative, which means a non-negative bias force F_0 exists.

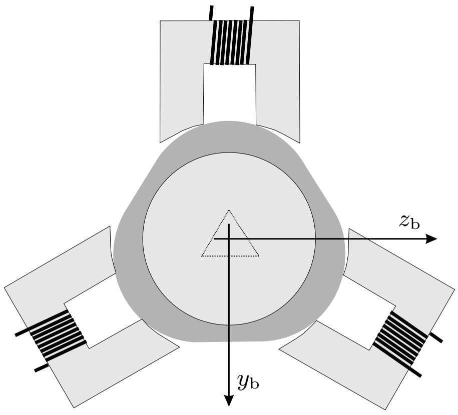

Fig. 3. Domain of operation of the Y-connected bearing. The rotor center may be positioned inside the triangle, the shaded region is the corresponding region covered by the rotor.

V. Experimental Results

Some experimental results obtained on the laboratory test-bench described in Section II may illustrate the usefulness of the proposed control designs and allow us to compare the configuration with Y-connected coils with the use of three independent controls.

Fig. 4 shows results obtained for an elliptic path with 5 and 10 μm axes with both control configurations. The spindle rotor is required to follow the same elliptic path in both bearing planes (cf. [1]). One may observe equally good tracking performance in both cases.

In the experiment reported in Fig. 5 a circular path with radius 35 μm has been prescribed, still in a parallel motion as above. With this larger deviation from the bearing center one may observe that negative currents may be required in order to meet the current constraint due to the Y-connection of the coils.

In all these experiments the spindle was rotating at 6000 rpm.

VI. Conclusion

High precision path tracking can be achieved with magnetically supported spindles. If the spindle is equipped with radial bearings with three phases in Y-connection standard commercial power electronics can be used. It has been shown how a controller can be designed with the two independent currents available in that case.

References

[1] St. Eckhardt and J. Rudolph. High precision synchronous tool path tracking with an AMB machine tool spindle. In *Proc. 9th International Symposium on Magnetic Bearings, Lexington*, 2004. Paper no. 109.

[2] J. Levine, J. Lottin, and J. C. Ponsart. A nonlinear approach to the control of magnetic bearings. *IEEE Trans. Contr. Syst. Technol.*, 4:524–544, 1996.

[3] J. von Löwis, J. Rudolph, J. Thiele, and F. Urban. Flatness-based trajectory tracking control of a rotating shaft. In *7th International Symposium on Magnetic Bearings, Zürich*, pages 299–304, 2000.

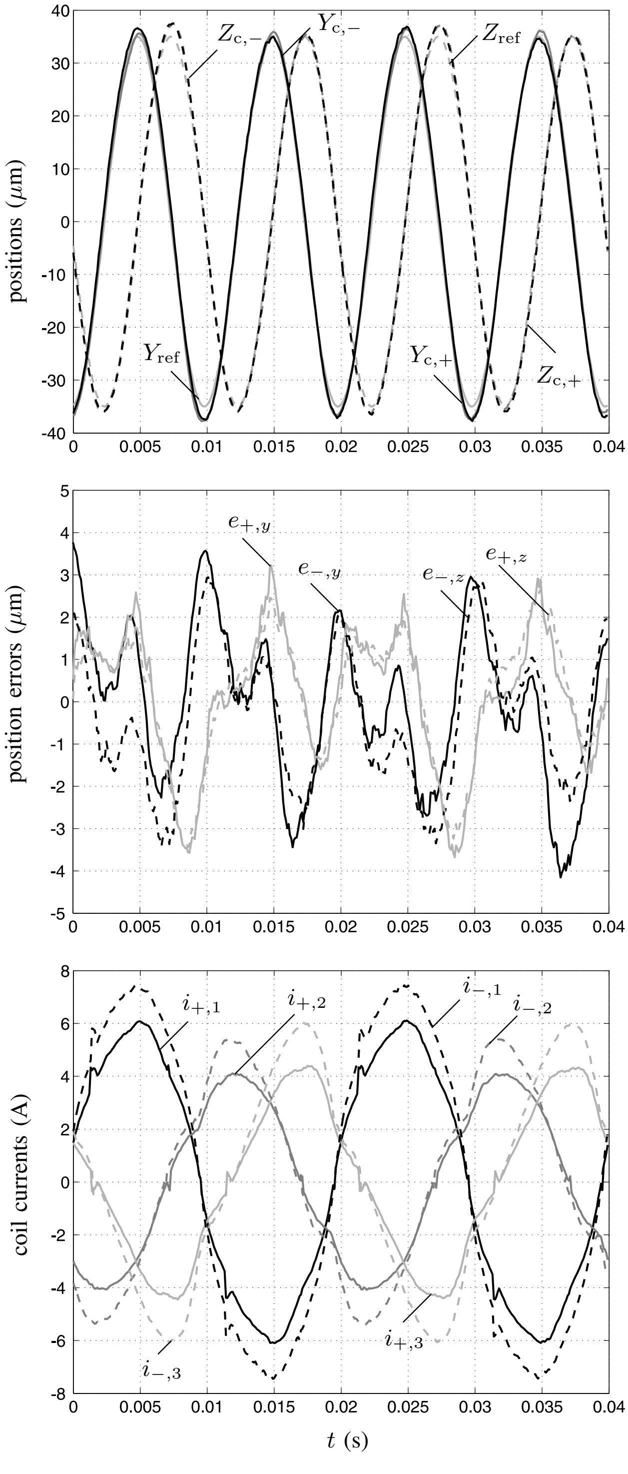

Fig. 5. Desired and actual circular paths with radius 35 μm in both bearing planes, corresponding tracking errors, and currents required with Y-connection.

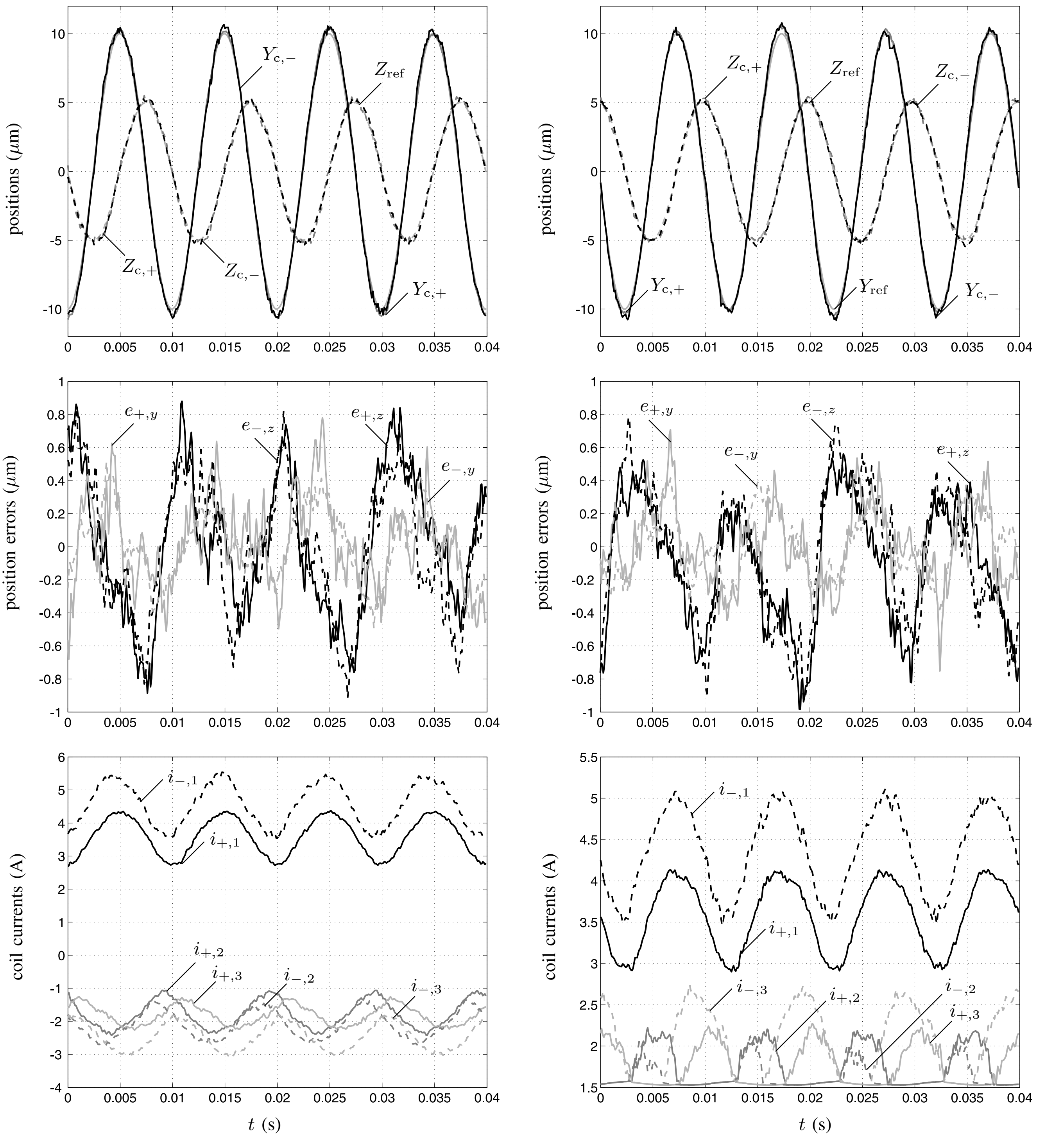

Fig. 4. Desired and actual elliptic paths with 5 and 10 μm axes in both bearing planes, tracking errors, and currents required; control using Y-connected currents (left) and three independent currents (right).